Evidence for new C-terminally truncated variants of α- and β-tubulins

Chrystelle Aillaud[a,b], Christophe Bosc[a,b], Yasmina Saoudi[a,b], Eric Denarier[a,b,c], Leticia Peris[a,b], Laila Sago[d], Nicolas Taulet[e], Adeline Cieren[a,b], Olivia Tort[f,g,h,i], Maria M. Magiera[g,h,i], Carsten Janke[g,h,i], Virginie Redeker[d,j], Annie Andrieux[a,b], and Marie-Jo Moutin[a,b,*]

[a]Université Grenoble Alpes, Grenoble Institut des Neurosciences, GIN, F-38000 Grenoble, France; [b]Inserm, U1216, F-38000 Grenoble, France; [c]CEA, BIG-GPC, F-38000 Grenoble, France; [d]Service d'Identification et de Caractérisation des Protéines par Spectrométrie de masse, CNRS, 91198 Gif-sur-Yvette, France; [e]Centre de Recherche de Biochimie Macromoléculaire, CNRS, 34293 Montpellier, France; [f]Institut de Biotecnologia i de Biomedicina, Department of Biochemistry and Molecular Biology, Universitat Autònoma de Barcelona, 08193 Bellaterra (Barcelona), Spain; [g]Institut Curie, 91405 Orsay, France; [h]Paris Sciences et Lettres Research University, 75005 Paris, France; [i]Centre National de la Recherche Scientifique, UMR3348, 91405 Orsay, France; [j]Paris-Saclay Institute of Neuroscience, CNRS, 91198 Gif-sur-Yvette Cedex, France

ABSTRACT **Cellular α-tubulin can bear various carboxy-terminal sequences: full-length tubulin arising from gene neosynthesis is tyrosinated, and two truncated variants, corresponding to detyrosinated and Δ2 α-tubulin, result from the sequential cleavage of one or two C-terminal residues, respectively. Here, by using a novel antibody named 3EG that is highly specific to the –EEEG C-terminal sequence, we demonstrate the occurrence in neuronal tissues of a new αΔ3-tubulin variant corresponding to α1A/B-tubulin deleted of its last three residues (EEY). αΔ3-tubulin has a specific distribution pattern: its quantity in the brain is similar to that of αΔ2-tubulin around birth but is much lower in adult tissue. This truncated α1A/B-tubulin variant can be generated from αΔ2-tubulin by the deglutamylases CCP1, CCP4, CCP5, and CCP6 but not by CCP2 and CCP3. Moreover, using 3EG antibody, we identify a C-terminally truncated β-tubulin form with the same –EEEG C-terminal sequence. Using mass spectrometry, we demonstrate that β2A/B-tubulin is modified by truncation of the four C-terminal residues (EDEA). We show that this newly identified βΔ4-tubulin is ubiquitously present in cells and tissues and that its level is constant throughout the cell cycle. These new C-terminally truncated α- and β-tubulin variants, both ending with –EEEG sequence, are expected to regulate microtubule physiology. Of interest, the αΔ3-tubulin seems to be related to dynamic microtubules, resembling tyrosinated-tubulin rather than the other truncated variants, and may have critical function(s) in neuronal development.**

Monitoring Editor
Kerry S. Bloom
University of North Carolina

Received: Mar 10, 2015
Revised: Dec 8, 2015
Accepted: Dec 22, 2015

INTRODUCTION

Tubulin is subject to a large number of posttranslational modifications that are evolutionarily conserved. Most of these modifications generate chemical marks at the C-terminal tail of tubulin that project outside microtubules and might, by regulating interactions with protein partners, select microtubules for specific cellular functions (Janke and Bulinski, 2011). Among these modifications is the cycle

This article was published online ahead of print in MBoC in Press (http://www.molbiolcell.org/cgi/doi/10.1091/mbc.E15-03-0137) on January 6, 2016.

C.A. performed and analyzed most of the experiments. C.B. performed the cloning of α-tubulin variant expression constructs. Y.S. and A.C. were involved in initiation of the project and with immunocytochemistry. L.S. and V.R. performed mass spectrometry. N.T. prepared synchronized HeLa cells. L.P. supervised neuronal cultures. E.D. helped with image quantification. O.T. and C.J. obtained the active CCP2 and CCP3 expression plasmids. M.M. provided TTLL1-knockout animal tissues. M.J.M. supervised the study and wrote the article. A.A., V.R., C.B., and E.D. participated in writing the article.

*Address correspondence to: Marie-Jo Moutin (moutinm@univ-grenoble-alpes.fr).

Abbreviations used: αΔ2/αΔ3-tubulin, α-tubulin truncated of two/three C-terminal amino acids; βΔ4-tubulin, β-tubulin truncated of four C-terminal amino acids; CCP, cytosolic carboxypeptidase.

of tyrosine removal and re-addition at the C-terminus of α-tubulin and the further cleavage of the penultimate glutamate, leading to the formation of α-tubulin truncated of two C-terminal amino acids (αΔ2-tubulin; Paturle-Lafanechere *et al.*, 1991). Another modification that generates a huge variety of C-terminal tail versions is the enzymatic polyglutamylation of both α and β subunits. This modification consists in addition of glutamate chains on the lateral chain of specific glutamate residues present in the primary sequences of the C-terminal region of tubulins (for review, see Janke and Bulinski, 2011).

The cycle of detyrosination/tyrosination involves two enzymes: an unidentified peptidase (tubulin carboxypeptidase [TCP]) producing detyrosinated tubulin, and a ligase that re-adds the tyrosine (tubulin tyrosine ligase [TTL]). TTL was discovered in 1993 (Ersfeld *et al.*, 1993) and shown to be essential for neuronal organization and tumor growth obstruction (Lafanechere *et al.*, 1998; Erck *et al.*, 2005). Polyglutamylation is generated by two families of enzymes: the glutamylase family, which has nine TTL-like enzymes (Janke *et al.*, 2005; van Dijk *et al.*, 2007), and the deglutamylase family, which includes six cytosolic carboxpeptidases (CCPs; Rogowski *et al.*, 2010; Moutin *et al.*, 2011; Tort *et al.*, 2014). Polyglutamylases differ in their preference for α- or β-tubulins and also for either side-chain initiation or elongation. Deglutamylases can either remove the branch points of the glutamate side chains from the tubulin backbones or hydrolyze peptide bonds between glutamate residues of linear chains. Deglutamylases were also shown to cleave the C-terminal glutamate from detyrosinated tubulin to generate αΔ2-tubulin (Rogowski *et al.*, 2010; Tort *et al.*, 2014).

The understanding of the molecular functions of each of these modifications in cells has progressed in recent years. The C-terminal tyrosine of α-tubulin was shown to be crucial for positioning of CAP-Gly proteins at microtubule plus ends and essential for proper functioning of depolymerizing motors of the kinesin-13 family (Badin-Larcon *et al.*, 2004; Peris *et al.*, 2006; 2009; Bieling *et al.*, 2008). Detyrosinated tubulin has been shown to regulate the binding and motor activity of processive kinesin-1 in cells (Liao and Gundersen, 1998; Dunn *et al.*, 2008; Cai *et al.*, 2009). An effect of microtubule detyrosination on processive motor functioning was also shown by in vitro experiments (Kaul *et al.*, 2014; Sirajuddin *et al.*, 2014). However, the regulation mechanism of this modification on motor transport is controversial. No molecular role has been determined for αΔ2-tubulin. Because it accumulates in differentiated cells, it was proposed to irreversibly lock microtubules in a detyrosinated state, thus helping to permanently stabilize them (Paturle-Lafanechere *et al.*, 1994). Polyglutamylation was shown to stimulate spastin-mediated microtubule severing and thus to participate in regulating microtubule dynamics and stability (Lacroix *et al.*, 2010). Controlling the extent of polyglutamylation of tubulins is critical for neuron survival, as shown by studying *pcd* (Purkinje cell degeneration) mice, which lacks functional CCP1 (Rogowski *et al.*, 2010). In these mice, tubulin hyperglutamylation leads to massive degeneration of particular neuron species.

In the brain, tubulins are very abundant and very heterogeneous, and this is essentially due to the presence of several tubulin isotypes arising from several genes and their polyglutamylation and detyrosination-linked modifications (Edde *et al.*, 1990; Alexander *et al.*, 1991; Redeker *et al.*, 1992, 1996, 1998; Redeker, 2010; Rudiger *et al.*, 1992, 1995; Mary *et al.*, 1994). Microtubules from neurons are known to carry elevated levels of polyglutamylated α- and β-tubulins (for review, see Janke and Bulinski, 2011), as well as high levels of detyrosinated and Δ2α-tubulin (Paturle-Lafanechere *et al.*, 1994; Redeker *et al.*, 1996). Because αΔ2-tubulin ends with a glutamate residue and some deglutamylases of the CCP family were shown to be able to cleave this residue in in vitro experiments (Berezniuk *et al.*, 2012, 2013), we wondered whether a new variant corresponding to α-tubulin truncated of three C-terminal amino acids (αΔ3-tubulin) could exist in cells and tissues. We therefore developed an antibody against this putative form of α-tubulin, which we showed is highly specific to the –EEEG C-terminal sequence. Using this antibody, we demonstrated for the first time the occurrence of a Δ3 form of α1A/B-tubulin in the brain under physiological conditions. Our novel antibody also allowed us to identify a new β-tubulin variant ending with the same C-terminus as αΔ3-tubulin and corresponding to the C-terminally truncated β2A/B-tubulin, as demonstrated by mass spectrometry. Thus we showed that both α- and β-tubulin are broadly modified by C-terminal amino acid truncation.

RESULTS

3EG, a new antibody specific to the –EEEG C-terminal sequence

To study the possible occurrence of a new variant of α-tubulin missing its three C-terminal amino acids in cells and tissues, we developed polyclonal antibodies directed against peptide GEGEEEG, corresponding to the seven terminal amino acids of α1A/B-tubulin without the EEY C-terminal tail. Sera from rabbits were tested for dilution and specificity by both Western blotting and immunocytochemistry.

The new antibodies (called 3EG), together with anti–tyrosinated α-tubulin (Wehland and Willingham, 1983), anti–detyrosinated α-tubulin, and anti–Δ2α-tubulin (Paturle-Lafanechere *et al.*, 1994) antibodies, were tested by Western blots on extracts of HEK293T cells expressing different α-tubulins varying in their C-terminus and fused to mCherry at their N-terminus. Anti–total α-tubulin (αtot; Erck *et al.*, 2005) was used as control of expressed mCherry–α-tubulins (95 kDa). As shown in Figure 1A (and quantified in Supplemental Table S1), each antibody is specific, and 3EG antibody is exclusively sensitive to αΔ3-tubulin. Faint bands are observed with anti-αTyr and anti-αΔ2 using extracts of cells expressing mCherry–αdeTyr-tubulin. They are very probably the result of endogenous TTL or CCP, respectively, adding a tyrosine residue or cleaving a glutamate residue on the mCherry-tubulin.

To further characterize the sequence specificity of the 3EG antibody, we examined the effect of different epitope mutations, allowing us to examine the reactivity of the antibody for the proteins from the seven α-tubulin genes (Figure 1B). Figure 1C illustrates that this novel antibody recognizes the four residues EEEG, with the glycine residue carrying the COOH. Changing the upstream glycine to a glutamate (using mCherry-αEEEEG) does not alter antibody reactivity. In contrast, modifying the two first glutamate residues of the EEEG motif leads to disappearance (as with mCherry-αGDDEG, -αGAEEG, and -αGENEG) or large reduction (as in the case of mCherry-αGEDEG) of staining. Figure 1B also shows that the C-terminal residue has a major antigenic character. Indeed, the antibody does not stain α-tubulin ending with an alanine instead of a glycine residue (a mutation that chemically represents only a small change of the lateral chain).

We also tested the 3EG antibody in immunocytochemistry experiments. We transfected fibroblasts with mCherry–αΔ3-tubulin and its mutated forms. We obtained comparable results to those observed by Western blot: 3EG was highly specific to fusion proteins ending with EEEG (Figure 1D; not all mutations are shown). Nonetheless, the antibody gave no signal with mCherry–α-GEDEG, in contrast to the slight staining obtained in the Western blot.

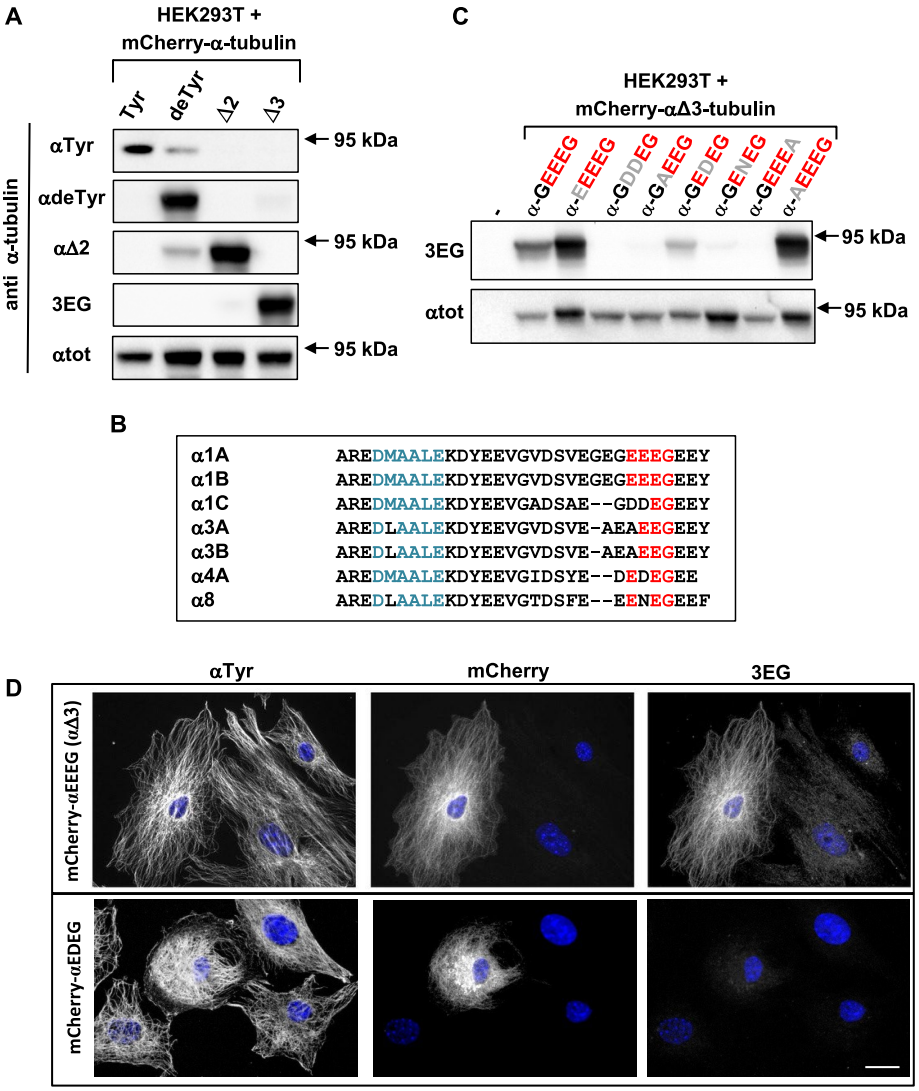

FIGURE 1: A new antibody specific to the –EEEG protein C-terminus, named 3EG. (A, C) Immunoblot of protein extracts from HEK293T cells expressing different forms of 95-kDa α-tubulin fused to mCherry at their N-terminus. Expression levels were controlled with αtot antibody. Antibodies recognizing either the unmodified C-terminal α-tubulin tail (tyrosinated tubulin) or its processed versions (detyrosinated or Δ2- or Δ3-tubulin) were used in A, and 3EG antibody was used in C to assay mutation (gray) of the Δ3-tubulin epitope (red). Quantification of the data in A is presented in Supplemental Table S1. (B) Alignment of mouse α-tubulin C-termini. Epitope of αtot antibody in blue; conserved amino acids from the –EEEG C-terminal sequence in red. (D) Immunocytochemistry of MEFs transfected with mCherry–αΔ3-tubulin and a mutated form of this protein ending with EDEG instead of EEEG. Scale bar: 20 μm.

Taken together, our results show that the new antibody we developed is highly specific to –EEEG C-termini (and was therefore named 3EG) and can be used in Western blot and immunocytochemistry experiments. Thus, although C-termini of α-tubulin genes share many amino acids, α1A/B, and to a lesser extent α4A, are the only ones stained by 3EG in Western blots, and only α1A/B is marked by 3EG in immunocytochemistry (Figure 1C). We thus used the 3EG antibody to examine by Western blot the possible occurrence of endogenous αΔ3-tubulins in mouse cells and tissues.

Evidence for αΔ3-tubulin in the brain and neurons

We prepared crude protein extracts from several organs of adult and neonate mice, including the brain, skeletal muscle, heart, kidney, stomach, and spleen. We also extracted proteins from brains at different ages and from different brain structures. Among all tissues tested, αΔ3-tubulin is present only in the brain in both neonates (Figure 2A) and adults. Moreover, αΔ3-tubulin is present in all brain regions analyzed (Supplemental Figure S1; neonate brain).

Surprisingly, in all tissues studied, we detected another protein that also reacts with 3EG antibody below the α-tubulin region, which thus does not correspond to αΔ3-tubulin (Figure 2A). We characterized this other protein as β-tubulin, as will be shown later. In most of the following figures for αΔ3-tubulin, the lower, β-tubulin band is not shown.

Analysis of αΔ3-tubulin occurrence in different cell types, including fibroblasts, astrocytes, and neurons prepared from either the hippocampus or brain cortex, showed that αΔ3-tubulin is solely present in neurons (Figure 2B). We studied its amount in hippocampal neurons at different days of differentiation in vitro (DIV; Figure 2C), from 3 to 21 DIV. We found that αΔ3-tubulin level was elevated from 3 to 14 DIV (corresponding to the time of axogenesis and then dentritogenesis of these neuronal cells) and largely decreases at 21 DIV. In contrast, αΔ2-tubulin is more abundant in differentiated neurons, as already described (Lafanechere and Job, 2000). We found that, in hippocampus neurons, the αΔ2-tubulin level significantly increases at 14 DIV and is still much higher at 21 DIV, when spinogenesis occurs.

We examined the presence of αΔ3-tubulin in the brain from embryonic day 13.5 (E13.5) to adult. Figure 2D shows a typical Western blot, and Figure 2E shows the quantification of the blots. We find that αΔ3-tubulin tends to have higher levels in the brain during embryonic stages and around birth and decreases later. In the adult brain, the level of αΔ3-tubulin is approximately three times lower than around birth. In contrast, the αΔ2-tubulin level increases in brain tissue throughout life, from the embryonic stage to adulthood. In the adult brain, the amount of αΔ2-tubulin is ~4 times the amount at birth and >10 times the amount at E13.5.

Status of the C-terminal truncations of the α-tubulin C-terminus in the brain

To further characterize α-tubulin species present in the brain, we quantified their distribution. Equal quantities of protein extracts from neonate and adult brains were subjected to immunoblot analysis with antibodies recognizing either the unmodified C-terminal α-tubulin tail (tyrosinated tubulin) or its processed versions (detyrosinated, αΔ2-, or αΔ3-tubulin; Figure 2F). Extracts from HEK293T cells transfected with the corresponding forms of mCherry-α-tubulin were coanalyzed (Supplemental Figure S2). The αtot antibody was used for equal loading of brain extracts or of HEK293T extracts

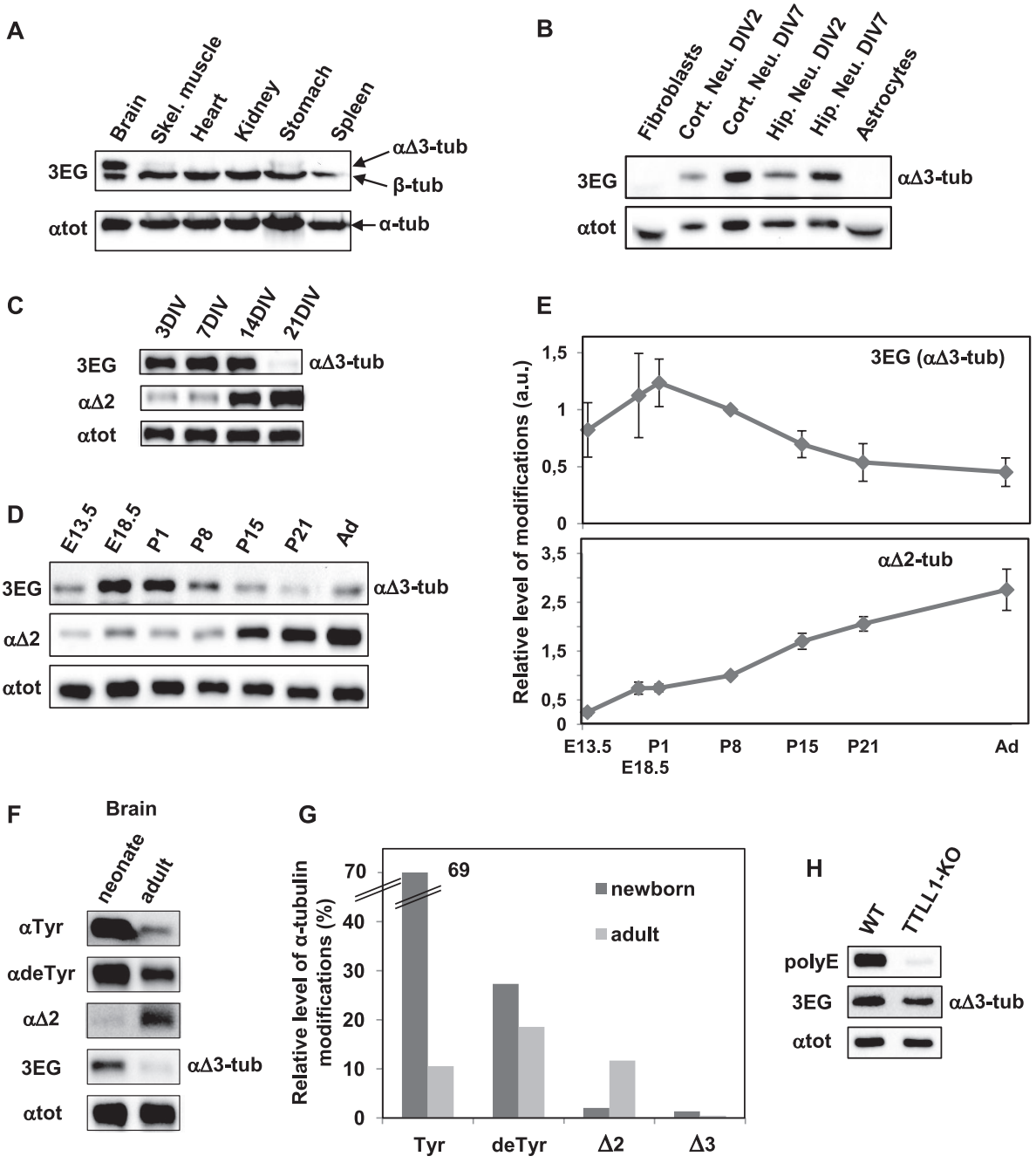

FIGURE 2: αΔ3-Tubulin, a neuronal variant enriched around mouse birth. Equal quantities of proteins extracted from various tissues and cell types were subjected to immunoblot analysis. Protein levels were controlled using αtot antibody. (A) Immunoblot of crude protein extracts from the indicated neonate mouse tissues. (B) Immunoblot of protein extracts from the indicated cell types, including cortical and hippocampal neurons cultured 2 or 7 DIV. (C) Immunoblot of hippocampal neurons at different stages of culture. (D) Immunoblot of crude protein extracts from mouse brains at different stages of development, including E13.5 and E18.5, postnatal days 1, 8, 15 and 21 (P1–21), and adult (Ad). Mixes of four or five half-brains were used at each developmental stage. (E) Quantitative analysis of three immunoblots for αΔ3 and of five immunoblots for αΔ2 realized as in D with brain protein extracts. In each immunoblot, values obtained were normalized to the value obtained at P8. Error bars indicate SEM; a.u., arbitrary units. (F) Immunoblot of protein extracts from neonate (P1) and adult mouse brains (same extracts as in D). These samples were coanalyzed with extracts from HEK293T cells transfected with the various mCherry–α-tubulin variants (Supplemental Figure S2). (G) Quantitative analysis of immunoblots such as those presented in Supplemental Figure S2. Mixtures of five neonate brains and five adult half-brains were analyzed in two series of Western blots. The plotted values represent the percentages of the different forms of α-tubulin in brains estimated after normalization to total α-tubulin levels (with αtot antibody) and to antibody sensitivity (using modified mCherry–α-tubulins) as explained in *Materials and Methods*. (H) Immunoblot of crude protein extracts from wild-type (WT) and TTLL1-knockout mouse brains.

expressing the mCherry-tagged α-tubulin variants. This experiment provides an estimate of the sensitivity of each tested antibody based on the immunoblot signal of the corresponding mCherry-tagged variant (Supplemental Figure S2) and then allows the approximation of the quantity of each variant of α-tubulin in the extracts (Figure 2, F and G). We estimated that tyrosinated, detyrosinated, αΔ2-, and αΔ3-tubulin variants, respectively, correspond to 69, 27, 2, and 1.3% of the total α-tubulin present in the neonate mouse brain. In adult brain tissue, α-tubulin variants were estimated as being divided into 25% tyrosinated, 45% detyrosinated, 28% αΔ2, and 1% αΔ3 of the total α-tubulin.

Because tubulin polyglutamylation is high in the adult brain and occurs in the vicinity of the sequence recognized by the 3EG antibody, we wondered whether this might affect the 3EG signal. We thus quantified the amount of 3EG signal in TTLL1-knockout brain extracts, which exhibit very low levels of glutamylation (Janke *et al.*, 2005), and observed no difference from wild-type brain extracts (Figure 2H). In controls, the tubulin polyglytamylation revealed by the polyE antibody almost completely disappeared from TTLL1-deficient extracts. Thus polyglutamylation does not alter 3EG antibody binding to tubulins.

Taken together, our results demonstrate the physiological occurrence of αΔ3-tubulin in brain tissue and particularly in neuronal cells. Although this pool of α-tubulin is not abundant, it is present in the brain and neurons at very specific stages. It is noteworthy that in the neonate brain, αΔ3-tubulin is present in a similar quantity to that of αΔ2-tubulin.

Specificity of deglutamylases involved in processing α-tubulin primary chain

Considering that deglutamylases from the CCP family catalyze removal of glutamate side chains of α- and β-tubulins and also deglutamylation of detyrosinated α-tubulin to form αΔ2 (Rogowski *et al.*, 2010; Tort *et al.*, 2014), we tested their ability to produce the αΔ3-tubulin variant. We analyzed protein extracts from HEK293T cells coexpressing mCherry-tagged αΔ2 tubulin and each of the CCPs. Results are presented in Figure 3A, with analysis of mCherry-tagged α-tubulin (95 kDa) on the left and examination of endogenous α-tubulin (55 kDa) on the right. We find that CCP1, CCP4, CCP5, and CCP6 are competent to form αΔ3-tubulin from expressed mCherry–αΔ2-tubulin (Figure 3A, left, row 2). In contrast, CCP2 and CCP3 seem to lack this ability. As already described (Rogowski *et al.*, 2010; Tort *et al.*, 2014), all CCPs except CCP5 generate the αΔ2 variant from endogenous α-tubulin present in HEK293T cells (Figure 3A, right, top). Moreover, our data illustrate that only CCP1 and CCP6 are sufficiently efficient to form αΔ3-tubulin from endogenous α-tubulin (Figure 3A, right, row 2): these two enzymes sequentially remove the two glutamate residues from endogenous detyrosinated tubulin, producing αΔ2- and then αΔ3-tubulin.

We also studied the activity of two of the deglutamylases, CCP1 and CCP5, in generating the αΔ3 variant from αΔ2-tubulin by immunocytochemistry on fibroblasts from TTL-knockout mice. Compared with wild type, fibroblasts isolated from TTL-knockout animals contain high levels of detyrosinated α-tubulin, as shown previously (Peris *et al.*, 2006), and αΔ2-tubulin (Figure 3B). Hence they contain high amounts of substrate allowing αΔ3-tubulin formation. However, as in the wild-type fibroblasts (Figure 2B), the αΔ3-tubulin variant is not detected in the TTL-knockout fibroblasts (Figure 3B). Figure 3C shows that the expression of CCP5 (green fluorescent protein [GFP]–positive cells) induces an important increase in 3EG antibody labeling on microtubules (the same results were obtained with CCP1; unpublished data). Figure 3D shows an analysis of the fluorescence levels within cells expressing either CCP1 or CCP5 (GFP-positive cells) compared with the level within cells that do not express the enzymes (GFP-negative cells). Both CCP1 and CCP5 largely increase microtubule staining by 3EG antibody in TTL-knockout fibroblasts, reflecting their capacity to generate αΔ3-tubulin. However, these two enzymes differ in their ability to form αΔ2-tubulin, as observed when studying their action on detyrosinated mCherry-tagged α-tubulin. Whereas CCP1 is able to process mCherry-deTyr-tubulin to generate the mCherry-αΔ2 variant, CCP5 is not competent (Supplemental Figure S3)

On the basis of all of these data, we conclude that CCP1, CCP4, and CCP6 are able to form αΔ2-tubulin from detyrosinated tubulin (cleavage of E-E) and αΔ3-tubulin from αΔ2-tubulin (cleavage of G-E). Thus, unpredictably, these three enzymes are capable of cleaving both E-E and G-E bonds. CCP2 and CCP3 are able to generate αΔ2-tubulin but seem incompetent to produce αΔ3-tubulin, and thus cleave E-E but not G-E bonds. CCP5, which is incompetent to cleave between two glutamates residues on the primary chain of α-tubulin to form αΔ2-tubulin, is efficient to cut between a glycine and a glutamate to generate αΔ3-tubulin from αΔ2-tubulin. Hence CCP2/3 and CCP5 seem to have different cleavage site preference (G-E vs. E-E), whereas CCP1/4/6 do not. Figure 3F summarizes these results.

We then wondered whether stabilizing microtubules could influence the generation of truncated variants and CCP activities as in the case of TCP. It is indeed well known that when living cells are incubated in the presence of the stabilizing drug paclitaxel, microtubules become more detyrosinated due to the action of TCP (Wehland and Weber, 1987; Contin and Arce, 2000). Detyrosinated tubulin represents the initial substrate for αΔ3-tubulin formation by CCPs, being first transformed in αΔ2-tubulin and subsequently in αΔ3-tubulin. We examined the effect of stabilizing microtubules with paclitaxel on the formation of the truncated variant levels using wild-type and TTL-knockout fibroblasts, the latter already containing a high amount of αΔ2-tubulin. We found that although incubation with 15 μM paclitaxel for 2 h induced a significant increase of αdeTyr-tubulin in both types of cells, neither αΔ2-tubulin formation nor αΔ3-tubulin formation was observed (Figure 3B). We obtained comparable results when using HEK293T cells expressing CCP1 subjected to the same drug treatment for 2 h (unpublished data). Thus, stabilizing microtubules for 2 h does not activate the CCP enzymes in charge of αΔ2- and αΔ3-tubulin formation, in contrast to what is observed with TCP. Given that activities of CCPs expressed in these cells are low (Rogowski *et al.*, 2010), we then tested the effect of paclitaxel added for a long time at lower concentrations (50–200 nM) on HEK293T cells expressing CCP1. We added the drug 2 h after CCP1 transfection and for 24 h. In this latter case, we observed both an increase of αΔ2-tubulin and a decrease of αΔ3-tubulin produced by the enzyme (Figure 3E, 50 nM paclitaxel). Hence generation of the truncated variants by CCP enzymes most probably relies on complex mechanisms related, at least in part, to microtubule dynamics. The reduction of these dynamics produces antagonistic effects on the generation of αΔ2-tubulin and αΔ3-tubulin.

β-Tubulin can be shortened at its C-terminus: evidence for ubiquitous βΔ4 variant

In all tissues (Figure 2A) or cells (Figure 4A) studied, we detected a protein band reacting with 3EG antibody just below the α-tubulin band, which thus does not correspond to αΔ3-tubulin. Migration of the two bands stained by the antibody is sensitive to the purity of the SDS used, as bands were effectively separated when less-pure

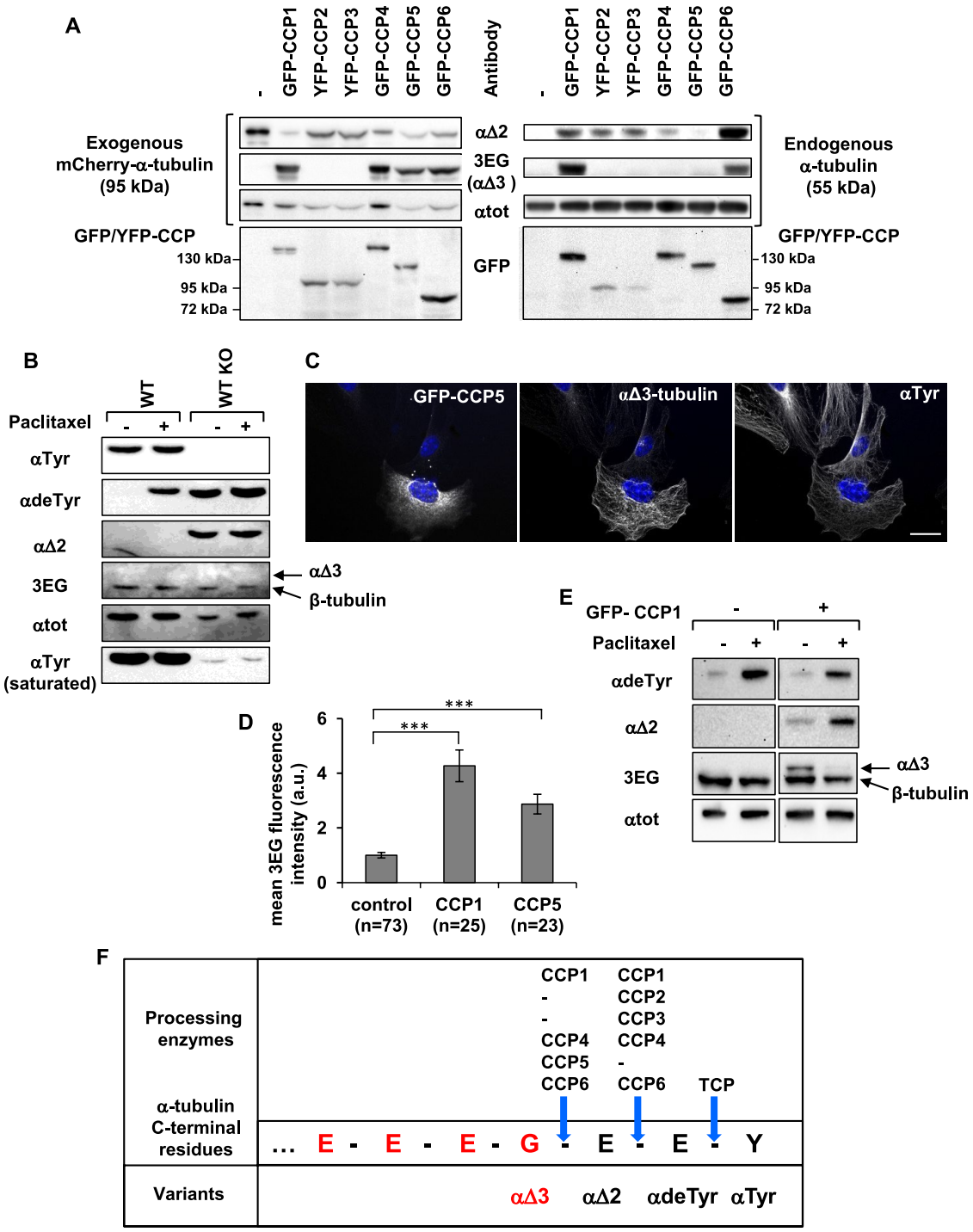

FIGURE 3: Specificity of CCP enzymes in producing αΔ2 and αΔ3. (A) Immunoblot of protein extracts from HEK293T cells coexpressing each GFP- or yellow fluorescent protein (YFP)–tagged CCP and mCherry–αΔ2-tubulin. Analysis of mCherry–α-tubulin (left) and endogenous α-tubulin (right). (B) Immunoblot of protein extracted from WT and TTL-knockout (TTL KO) fibroblasts after incubation with dimethyl sulfoxide (DMSO: control) or paclitaxel (15 μM) for 2 h. TTL KO cells contain high levels of detyrosinated and αΔ2-tubulin, but no αΔ3-tubulin is detected. The reactive 3EG band corresponds to β-tubulin (Figure 4). (C) Immunocytochemistry of TTL KO fibroblasts transfected with GFP-CCP5 and immunostained with anti–αTyr-tubulin and 3EG antibody. Scale bar: 20 μm. CCP5 leads to the formation of αΔ3-tubulin. (D) Quantitative analysis of immunocytochemistry experiments as in C using TTL KO fibroblasts transfected with either GFP-CCP1 or GFP-CCP5. Fluorescence was measured as explained in *Materials and Methods*. (E) Immunoblot of protein extracted from HEK293T cells expressing GFP-CCP1 or not after incubation with DMSO (control) or paclitaxel (50 nM) for 24 h. (F) Schematic representation of the C-terminal amino acids of α1A/B-tubulin, 3EG epitope (red), and processing enzymes associated with the generation of the variants.

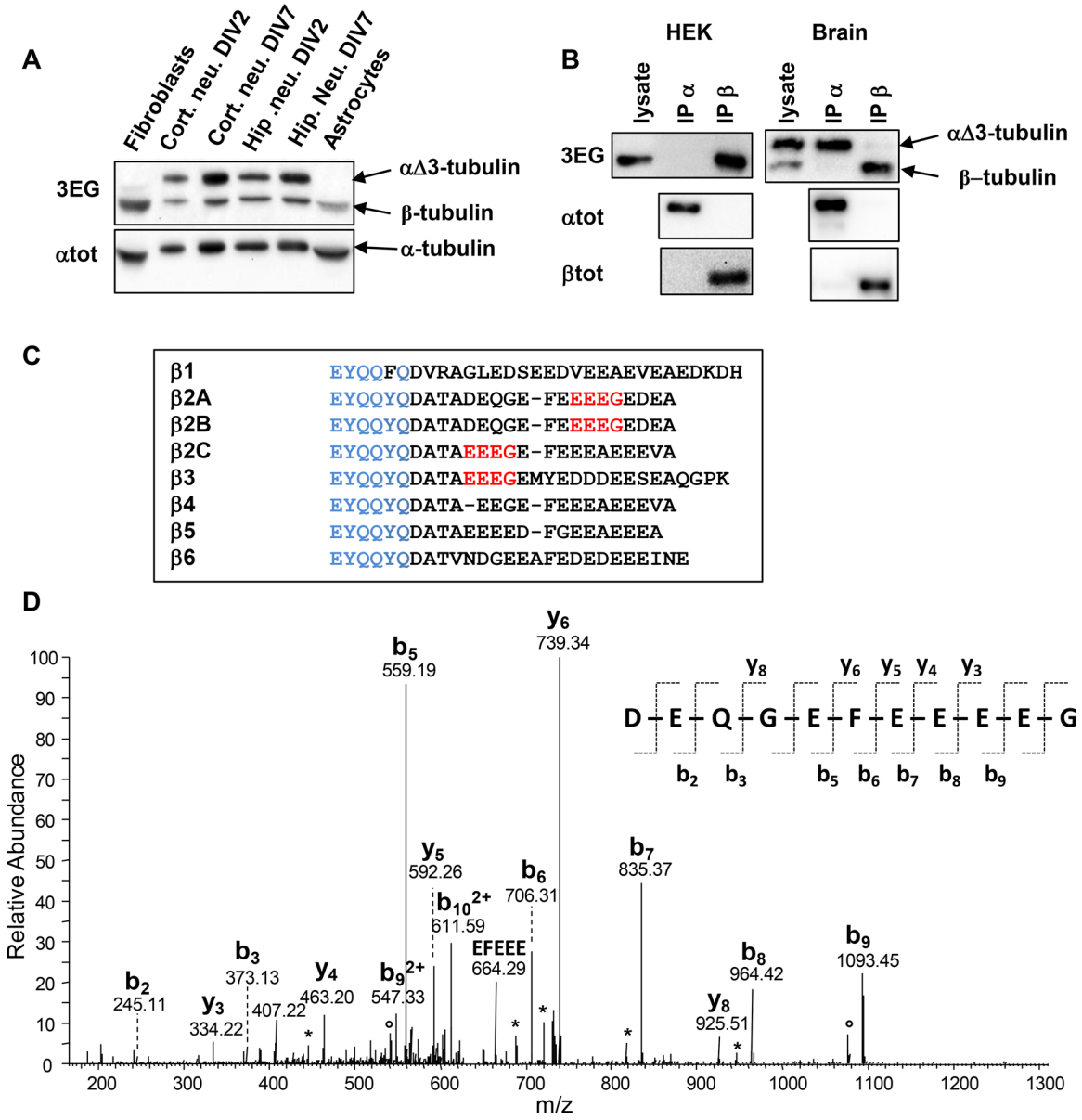

FIGURE 4: Evidence for a ubiquitous truncated form of β-tubulin. (A) Immunoblot of crude extracts from the indicated mouse tissues (same experiment as Figure 2B, but with the lower protein bands included). Protein levels were controlled using αtot antibody. (B) Immunoprecipitation of endogenous α- and β-tubulins from HEK293T cells and neonate mouse brain using αtot (IP α) and βtot (IP β) antibodies and analysis with 3EG antibody. The quality of immunoprecipitations was controlled using αtot and βtot antibodies together with mouse TrueBlot secondary antibodies. (C) Alignment of C-termini from the eight mouse β-tubulin isotypes. The βtot antibody epitope is in blue, and the 3EG epitope is in red. (D) Identification of the C-terminal peptide of the truncated β2A/B-tubulin (ΔEDEA) from neonatal mouse brain. The MS/MS spectrum of the peptide ion with $m/z = 649.24$, corresponding to an experimental monoprotonated mass MH+ of 1296.4632 Da, is annotated. The *b*- and *y*-type fragments identified are indicated on the sequence of the C-terminal peptide DEQGEFEEEEG, with a theoretical mass MH+ of 1296.4630 Da. Loss of H_2O and NH_3 is labeled with asterisks and open dots, respectively.

SDS was used. This well-known comportment of α- and β-tubulins from the tubulin dimer (Best *et al.*, 1981) led us to suspect that the second protein stained by 3EG antibody could be β-tubulin. After purification of tubulins from adult and neonate brains by a cycle of microtubule assembly and disassembly, we found the same 3EG labeling, which strongly suggests that the two bands correspond to the two tubulin monomers (Supplemental Figure S4). To confirm our hypothesis, immunoprecipitation experiments with anti–α-tubulin (αtot) and anti–β-tubulin (βtot) antibodies were done on crude protein extracts from HEK293T cells and neonate brains. The assays were performed in experimental conditions allowing separation of the tubulin monomers, in medium containing Tris buffer as in Giraudel *et al.* (1998). Results presented Figure 4B show that the protein present in the lower 3EG band from both extracts is immunoprecipitated by the anti–β-tubulin antibody, whereas the αΔ3 variant from brain extract is immunoprecipitated by αtot. As illustrated

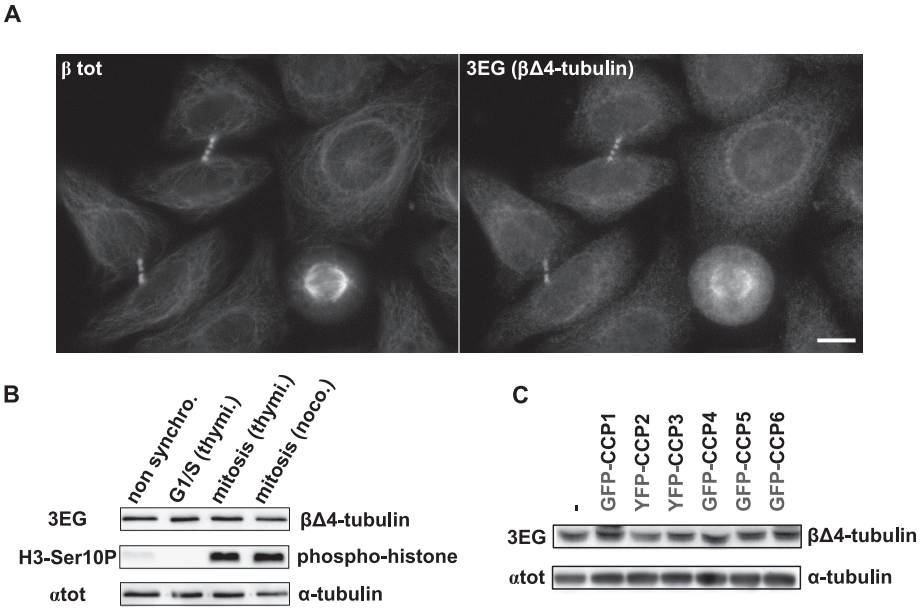

FIGURE 5: The novel β2A/B-tubulin variant βΔ4 evidenced in HeLa cells by 3EG antibody. (A) Immunocytochemistry of HeLa cells using 3EG and anti–β-tubulin antibody (βtot). Scale bar: 10 μm. (B) Immunoblot of protein extracts from nonsynchronized HeLa cells and from HeLa cells synchronized in G1/S or mitosis (see *Materials and Methods*). Cell synchronization was verified using a phosphohistone antibody (H3-Ser10P). Loaded proteins were standardized using αtot antibody, and the truncated β-tubulin form was analyzed with 3EG antibody. (C) Analysis of the β-tubulin band in protein extracts from HEK293T cells expressing GFP- or YFP-tagged CCPs (complementary analysis of the experiment in Figure 3A, right, including lower band).

Figure 4C, none of the β-tubulin isotypes encoded by the eight mouse genes contains an –EEEG sequence at its C-terminus. However, the sequence is present upstream within the C-terminal region of β2A/B-, β2C-, and β3-tubulin isotypes. To identify the β monomer subjected to C-terminal cleavage, we separated tubulins purified from neonate brains by SDS–PAGE. The protein band recognized by 3EG antibody and corresponding to β-tubulins was digested with AspN endoprotease. Peptides generated upon proteolysis were analyzed by mass spectrometry as described in *Materials and Methods*. We identified β1-, β2A/B-, and β3-tubulin isotypes in the mouse neonate brain, as previously observed in the rat neonate brain (Redeker, 2010). We detected the full-length C-termini of these three β-tubulin isotypes, predominantly nonglutamylated, but also monoglutamylated (β1, β2A/B, and β3) and biglutamylated (β2A/B and β3). By using a database of all possible truncated tubulin forms, we unambiguously identified a C-terminal peptide of the β2A/B-tubulin missing the four last amino acids, –EDEA (Figure 4D), named βΔ4-tubulin, which terminates with –EEEG residues and presents the epitope recognized by the 3EG antibody. This peptide was predominantly nonglutamylated, but a low-abundance monoglutamylated form was also identified by mass spectrometry. No other truncated C-terminal peptide of β-tubulin was detected.

We then used 3EG antibody in immunofluorescence experiments with cells that solely had the 3EG-reactive βΔ4-tubulin, such as astrocytes, fibroblasts, or HeLa cells, and observed that microtubule arrangements found in mitotic spindles and midbodies are clearly stained by the 3EG antibody (Figure 5A and Supplemental Figure S5). Because we clearly observed labeling in these specific microtubules structures, we investigated whether the cell cycle could regulate the level of C-terminally truncated β variants. However, HeLa cells synchronized in either G1/S or mitosis showed no 3EG labeling difference in Western blot experiments (Figure 5B), proving that the βΔ4-tubulin level is stable throughout the cell cycle.

Because the quantity of βΔ4-tubulin is not modified in HEK293T cells overexpressing CCPs (Figure 5C), these enzymes are most probably not involved in the production of the shortened β-tubulin variant.

Taken together, our data demonstrate for the first time the presence of a C-terminally truncated variant of β-tubulin ubiquitously distributed in cells and tissues (Figures 2A and 4A). This new form of tubulin is attributed to the β2A/B-tubulin isotypes and named βΔ4-tubulin.

Properties of the new truncated variants of tubulin in neurons

We examined the endogenous tubulin variants by immunofluorescence in cultured hippocampal neurons (2 DIV). Figure 6A illustrates that the 3EG immunoreactivity for both αΔ3- and βΔ4-tubulin is present in the whole neuron. Moreover, we observe a strong correlation of 3EG immunoreactivity with αTyr staining but not with αdeTyr and αΔ2 staining (Supplemental Figure S6, A [growth cone magnification] and B [quantification of modified-to-total α-tubulin ratio in the axon shaft and the growth cone]; this ratio changed between the axon and the growth cone when considering αdeTyr- and αΔ2-tubulins, but not when considering αΔ3- or αTyr-tubulins]). To assay the relationship between new tubulin variants and microtubule stability, we analyzed resistance to nocodazole of microtubules from the growth cone, which contains high levels of labile domains of tyrosinated microtubules, as well as stable domains of detyrosinated microtubules (Baas *et al.*, 1993; Brown *et al.*, 1993). The ratio of each tubulin variant signal to total α-tubulin signal was measured over time after nocodazole treatment (15 μM). As predicted, nocodazole-resistant microtubules were largely enriched in αdeTyr-tubulin over time, whereas their content in αTyr-tubulin decreased (Figure 6B). Only slight changes in αΔ2 and 3EG (including αΔ3- and βΔ4-tubulin) signals were detected in nocodazole-resistant microtubules. Thus 3EG-positive and αΔ2-positive microtubules seem to have moderate stability in the growth cone of hippocampal neurons.

To distinguish αΔ3-tubulin and βΔ4-tubulin species, we then examined the endogenous variants by Western blots. Their distribution between soluble and polymer pools was studied in 7 DIV hippocampus neurons in both the absence and presence of nocodazole (Figure 6C). Acetylated-tubulin, a marker of highly stable microtubules, was used as control. In the absence of nocodazole exposure, 97.4% of the signal for acetylated-tubulin was recovered in the microtubular fraction (Figure 6C, left). We found that αΔ3-tubulin is clearly enriched within the microtubular fraction, like αdeTyr-tubulin and αΔ2-tubulin (88–92%). Of interest, the new β-tubulin variant (βΔ4) was also principally retrieved within the polymer pool (87.7 ± 2.1%, mean ± SEM, $n = 3$). In contrast, only 70% of αTyr-tubulin was found in the microtubular pool and 30% in the soluble one. On adding 20 μM nocodazole for 30 min, we observed a significant loss of neuronal microtubules (28%, as estimated from immunoblotting with αtot antibody) and clear changes in α-tubulin species distribution between soluble and microtubular pools

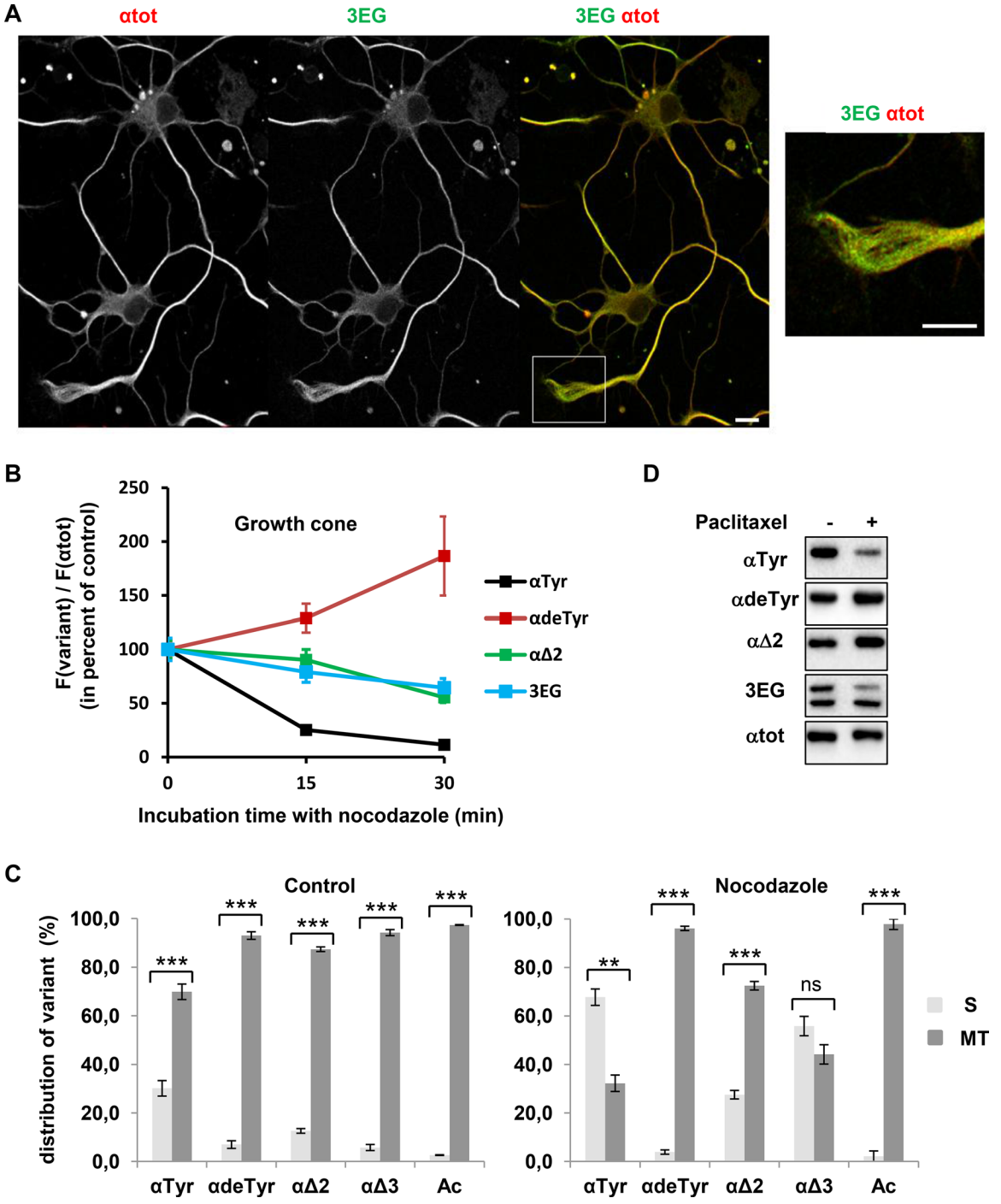

FIGURE 6: Properties of neuronal 3EG-positive microtubules and tubulins. (A) Immunofluorescence study of the distribution of microtubules bearing αΔ3- and βΔ4-tubulin (3EG-positive microtubules) in hippocampal neurons cultured 2 DIV. Scale bar, 10 μm. Inset, magnification of the growth cone. Distribution of microtubules bearing the other α-tubulin variants is shown in Supplemental Figure S6. (B) Time course of nocodazole (20 μM) resistance of microtubules from 2 DIV hippocampal neurons analyzed in the growth cone (mean ± SEM). Microtubule fluorescence signals were measured for a minimum of 31 neurons at each time of drug treatment. The fluorescence signal of each tubulin variant, *F*(variant), was normalized to the total α-tubulin fluorescence signal, *F*(αtot), which is an index of the remaining microtubules, and then was plotted as percentage of the value obtained in the absence of nocodazole (time 0). (C) Immunoblot analysis of the distribution of α-tubulin species between soluble (S) and microtubular (MT) fractions in 7 DIV hippocampal neurons in the absence (left) or presence of 20 μM nocodazole for 30 min (right). The S and MT protein extracts from neuronal cultures ($n = 3$) were obtained as in Audebert *et al.* (1993). Results are shown as mean values ± SEM. ***$p < 0.001$ and **$p < 0.01$, *t* test. (D) Immunoblot of protein extracted from 7 DIV hippocampal neurons after incubation with DMSO (control) or paclitaxel (15 μM) for 2 h.

(Figure 6C, right). As predicted, acetylated tubulin was recovered in the microtubular fraction (97.8%). The same fraction contained 96% of the αdeTyr-tubulin, 72.5% of the αΔ2-tubulin, 44.2% of the αΔ3-tubulin, and 30% of the αTyr-tubulin. Thus αΔ3-tubulin behavior under nocodazole treatment is closer to that of labile αTyr-tubulin than to that of stable αdeTyr-tubulin. Of interest, αΔ3-tubulin increases and persists in the soluble pool after drug treatment, suggesting irreversible modification within the cytosol.

To further analyze the relationship between microtubule dynamics and tubulin variants in hippocampal neurons, we performed experiments using paclitaxel. Neuron exposure to the stabilizing drug (15 μM) for 2 h induces clear changes in the α-tubulin variants: we observed a reduction of tyrosinated tubulin and αΔ3-tubulin and an accumulation of detyrosinated- and αΔ2-tubulin (Figure 6D). Thus the shutdown of tubulin dimer turnover between free tubulin and microtubules under paclitaxel exposure induces a loss of αΔ3-tubulin in cells (see also results in Figure 3E for HEK293T cells expressing CCP1).

Taken together, our results show that αΔ3-tubulin and βΔ4-tubulin are essentially found in the microtubular pool of neurons. They strongly suggest that microtubular dynamics is required for αΔ3-tubulin generation and/or maintenance.

DISCUSSION

In the present study, we developed a novel antibody highly specific to C-terminal –EEEG of proteins, which we named 3EG. This antibody detected two proteins among all mouse tissues and cells tested. We demonstrated that these proteins are novel C-terminally truncated variants of α- and β-tubulins.

In the neonate mouse brain, the most abundant of these two proteins reacting with 3EG corresponds to α1A/B-tubulin missing its last three amino acids. This truncated variant, named αΔ3-tubulin, was previously suspected to exist (Berezniuk *et al.*, 2012) because CCP1 produced in insect cells is able to generate it in vitro from purified porcine brain tubulin. Our work demonstrated for the first time the physiological existence of αΔ3-tubulin, its restricted presence in neuronal cells, and its enrichment in the brain around birth. It has been shown that in the adult rat brain, α1A/B-tubulin isotypes constitute ~85% of the α-tubulin subunit pool (of which 30% are tyrosinated and 70% are nontyrosinated), whereas isotype α4A represents 15% (predominantly nontyrosinated; Redeker, 2010). In neonates, however, only α1A/B tubulins were detected (Redeker, 2010). When truncated of three (α1A/B) or two (α4A) amino acids (Figure 1C), these brain α-tubulin isotypes all react with 3EG. The α1A- and α1B-tubulins are the only isoforms present in the neonate brain and are the source of αΔ3-tubulin at this stage. They might also be the tubulin isotypes having this modification in adult brains, even if a truncation of α4A cannot be excluded. Of interest, a Δ5 form of α-tubulin ending with the –EEEG C-terminal sequence was clearly revealed by mass spectrometry in *Toxoplasma gondii* (Xiao *et al.*, 2010). We tested the ability of the enzymes of the CCP family to produce αΔ3-tubulin and αΔ2-tubulin from mCherry–α1B-tubulin fusion protein; the results are summarized in Figure 3E. They are in agreement with recent data showing that CCP1 and CCP5 purified from sf9-infected cells can catalyze the formation of αΔ3-tubulin (Berezniuk *et al.*, 2013). In addition, we show that CCP4 and CCP6 are also able to cleave αΔ2-tubulin to generate αΔ3-tubulin and that CCP2 and CCP3 seem unable to catalyze this reaction. Our results are discrepant with those of Berezniuk *et al.* (2013) concerning the effect of CCP5 on the C-terminus of α-tubulin. Indeed, we clearly show here that CCP5 is not able to form αΔ2-tubulin from detyrosinated tubulin, whereas they concluded that this enzyme is able to process the concerned glutamate residue. The most probable explanation of this discrepancy relates to the tubulin isotype studied. Their observation was made on the α4A-tubulin isotype, whereas our results were obtained with α1B-tubulin (fused to mCherry). Therefore we give here the first indication that CCP deglutamylases (in the present case, CCP5) might be selective of the α-tubulin isotype for their activity on the primary chain of the protein. This might also be the case regarding CCP activity on glutamate side chains.

The second protein reacting with 3EG antibody was identified as a novel C-terminally truncated β-tubulin, as shown by both immunoprecipitation experiments and mass spectrometry analysis. Within neonate brains (in which β-tubulin is less polyglutamylated and thus easier to analyze), we identified a truncated form of β2A/B-tubulin that ends with –EEEG and results from the cleavage of the last four amino acids, –EDEA, from the full-length protein encoded by its gene. The β2A/B-tubulin isotypes were found in several tissues and represent the predominant isotypes in the nervous system, where they are expressed in both neurons and glia (Luduena, 2013). The newly discovered variant, named βΔ4-tubulin, is present in all mouse tissues and cells tested at low level (similar to αΔ3-tubulin, as observed from the intensity of both band signals obtained with 3EG antibody; Figures 2A and 4A). Although βΔ4-tubulin can be clearly observed by immunofluorescence when concentrated in mitotic spindles or midbodies, its level does not vary during the cell cycle. Because microtubules are bundling in such mitotic arrangements, we cannot distinguish between a specific or nonspecific enrichment of the new truncated tubulin variant in these structures.

Although truncation of the α-tubulin C-terminus was discovered some time ago and, since then, detyrosination/tyrosination of α-tubulin has been shown to play a vital role (Erck *et al.*, 2005), very few studies have described truncations in the C-terminal region of β-tubulins. To our knowledge, the work by Miller *et al.* (2008) is the only one describing truncated β-tubulin in mammals. They found evidence for the removal of the C-terminal alanine and the penultimate valine residues from β2C-tubulin in rat liver tissue (Miller *et al.*, 2008). β-Tubulin truncation was also observed in sea urchin. Indeed, a large amount (20%) of the β-tubulin from sea urchin sperm flagellar axonemes unexpectedly lacks the three carboxy-terminal residues –EAA encoded by its gene (Multigner *et al.*, 1996). Thus glutamate and aspartate, but also alanine and valine, residues appear to be cleaved from proteins encoded by β-tubulin genes. Carboxypeptidases capable of cleaving acidic residues, deglutamylases and deaspartylases, were recently discovered (Rogowski *et al.*, 2010; Tort *et al.*, 2014). Physiological substrates for deglutamylases, such as lateral chains of glutamates on tubulins and other proteins, and C-termini of α-tubulins have long been known. Our data indicate the first physiological substrate for deaspartylases: mammalian β2A/B-tubulin isotypes. The newly identified truncated variant of β-tubulin strongly argues for the existence of other enzymes allowing an increasing range of carboxy-terminal processing. In particular, because all of the processed β-tubulins end with an alanine (Multigner *et al.*, 1996; Miller *et al.*, 2008), dealaninases should very probably exist.

By the use of specific antibodies and a series of mCherry–α-tubulin isotypes as standards, we estimated the distribution of the diverse α-tubulin variants, αTyr, αdeTyr, αΔ2, and αΔ3, in the neonate and adult mouse brain (Figure 2G). For the already known variants (αTyr, αdeTyr, and αΔ2), our data for adult mouse brain are in good agreement with the data obtained by mass spectrometry using rat brains (Redeker *et al.*, 1998) and by a separation method using the bovine brain (Paturle *et al.*, 1989). In addition, our analyses show that the αΔ3 neuronal variant represents only a small portion (~1%) of the total amount of α-tubulin present in the neonate and adult

brain. It may thus be involved in very specific function(s) of the neuronal microtubules.

Surprisingly, the total amount of α-tubulin found in adults when adding all species corresponds to only 41% of the total amount of α-tubulin found in neonates. Indeed, we observed a decrease of all variants of α-tubulin except αΔ2 between neonate and adult tissue: tyrosinated tubulin decreases sevenfold, detyrosinated tubulin by 30%, and αΔ3 by threefold, whereas αΔ2-tubulin increases about sixfold. Two explanations can be considered to explain these results. First, some modification might occur in the adult brain (such as lateral polyglutamylation) that disturbs the binding of the α-tubulin C-terminus antibodies used in the present study (anti-tyrosinated, -detyrosinated, -Δ2, -Δ3). In such a case, however, it would be surprising that the level of αΔ2 would still increase as much as six times between neonate and adult tissues (Figure 2G). This is also unlikely because α-tubulin is already very glutamylated in neonate brains (Redeker, 2010) and we showed that polyglutamylation does not alter 3EG antibody binding to tubulin (Figure 2H). Thus the second, likelier explanation is that other unknown modification(s) of the α-tubulin C-terminus might occur in the adult brain and regulate C-terminal truncation.

The discovery of two novel C-terminally truncated variants of tubulins and, remarkably a truncated form of β-tubulin increases their diversity. These variants of α- and β-tubulins, which end with the same amino acids sequence, –EEEG, could share a common specific physiological significance. In neurons, αΔ3-tubulin and βΔ4-tubulin are essentially found in the microtubular pool. Of interest, αΔ3-tubulin is present on neuronal microtubules sharing properties with tyrosinated microtubules and not with microtubules bearing the other truncated α-tubulin species or the acetylated tubulin. Hence the neuronal microtubule network appears to be more heterogeneous in composition and turnover rate than previously described, when only tyrosinated and detyrosinated tubulins were known (Schulze *et al.*, 1987; Webster *et al.*, 1987). Although corresponding to a modified tubulin, the αΔ3 species seems to be related to dynamic microtubules. Microtubule turnover appears to be required for its generation and/or maintenance, in contrast to αΔ2-tubulin formation, which requires stable microtubules. To explain these properties, we can speculate that whereas αΔ2-tubulin may be generated by CCP enzymes on microtubules, the αΔ3 variant may be formed by these enzymes in the cytosol. It is of interest that levels of αΔ3-tubulin change with brain age, and it is mainly present before and around birth. Thus the αΔ3-tubulin species could have critical function(s) for neuronal development, most probably related to highly dynamic microtubules. The new αΔ3-variant could also confer specific properties on neuronal microtubules due to interaction with specific partners.

Deciphering precisely the function(s) of the new physiological αΔ3- and βΔ4-tubulin forms will be of crucial importance. This is also the case for the abundant neuronal αΔ2-tubulin (Paturle-Lafanechere *et al.*, 1991, 1994), for which specific functions remain to be identified.

MATERIALS AND METHODS

Mouse experiments

In compliance with the European Community Council Directive of November 24, 1986 (86/609/EEC), research involving animals was authorized by the Direction Départementale de la Protection des Populations, Préfecture de l'Isère, France (Permit 380711). Every effort was made to minimize the number of animals used and their suffering. This study was approved by the local ethics committee of the Grenoble Institut des Neurosciences. For tissue preparation or cell culture, mice were killed and organs were quickly dissected. TTL-knockout mice were first described in Erck *et al.* (2005) and TTLL1-knockout mice in Vogel *et al.* (2010).

Cell culturing

Hippocampal neurons and murine embryonic fibroblasts (MEFs) were prepared as previously described (Erck *et al.*, 2005). Astrocytes and cortical neurons were obtained from cerebral cortices of 18-d mouse fetuses and MEFs from 13-d mouse fetuses. Adherent HEK293T cells were maintained under standard conditions.

For the synchronization protocol, HeLa Kyoto cells were cultured in DMEM supplemented with 10% fetal bovine serum. Cells were nonsynchronized, synchronized in G1/S using double-thymidine block (2 mM), or synchronized in mitosis using either double-thymidine block released for 9 h or nocodazole block (100 ng/ml) released for 30 min. Mitotic cells were collected after release by mitotic shake-off. Cell extracts were obtained after lysis with buffer containing 50 mM 4-(2-hydroxyethyl)-1-piperazineethanesulfonic acid (pH 7.5), 150 mM NaCl, 1.5 mM $MgCl_2$, 1 mM ethylene glycol tetraacetic acid (EGTA), 1% IGEPAL CA-630, and protease inhibitors (Sigma-Aldrich, Taukkirchen, Germany). Protein concentration for lysate was determined using Bradford reagent (Sigma-Aldrich).

Antibodies

Primary antibodies used in this study are presented in Supplemental Table S2. The novel antibody (3EG) was produced in rabbits by using peptide C-GEGEEEG (α1A/B-tubulin C-terminus missing three amino acids) linked at its N-terminus to the keyhole limpet hemocyanin protein via the cysteine. The peptide C-terminus ends with COOH. Anti-rabbit, anti-mouse, and anti–guinea pig secondary antibodies tagged with either cyanine-5 or cyanine-3 were from Jackson ImmunoResearch (Newmarket, United Kingdom), and anti-rabbit, anti-mouse, and anti-guinea pig secondary antibodies tagged with horseradish peroxidase (HRP) were from Macherey Nagel (Hoerdt, France). Mouse TrueBlot ULTRA (anti-mouse immunoglobulin G–HRP) was from eBioscience (Paris, France).

Expression constructs and cell transfection

The GFP-CCP expression constructs used in the present study were described previously (Peris *et al.*, 2009; Rogowski *et al.*, 2010; Tort *et al.*, 2014). The α-tubulin variant constructs were generated by introducing mutations with PCR amplifications between the *Psh*AI and *Bam*HI restriction sites of α-tubulin cDNA (mouse α1A-tubulin tagged with mCherry; Supplemental Table S3). The various PCR products were cloned into templates by using the In-Fusion HD Cloning Kit (Ozyme, Montigny, France). All constructs were verified by sequence analysis.

Adherent HEK293T cells were transfected with jetPEI transfection reagent (Polyplus-Transfection, Illkirch, France). For cotransfections of mCherry–α-tubulin with CCPs (Figure 3 and Supplemental Figure S3), a 2:1 ratio was used. Murine embryonic fibroblasts were transfected using Amaxa Nucleofector kits (Lonza, Basel, Zwitzerland).

Western blotting

For Western blotting, cells were collected after 24 h of transfection when transfecting one plasmid and after 48 h when transfecting two plasmids. After washing with phosphate-buffered saline (PBS) medium at 37°C, cells were directly lysed in Laemmli buffer. Crude protein extracts from tissues were obtained by extraction in 100 mM 1,4-piperazinediethanesulfonic acid at pH 6.7, 1 mM EGTA, 1 mM $MgCl_2$, and protease inhibitors (Complete Mini EDTA-free; Roche Diagnostics, Meylan, France) using a FastPrep Instrument (MP Biomedicals, Illkirch, France). Cell remnants were eliminated by

10 min of centrifugation at 10,000 × *g*, and Laemmli buffer was added. Proteins were resolved on 10% SDS–PAGE, followed by electrotransfer onto Immobilon P sheets (Millipore, St Quentin en Yvelines, France). Two commercial SDS preparations were used (Sigma-Aldrich L5750 and L4509), with the less pure one allowing clear separation of α- and β-tubulins, as previously observed (Best *et al.*, 1981). Primary antibodies (Supplemental Table S2) were incubated, and the blots were then stained with secondary antibodies coupled to HRP (1:5000), followed by detection by chemiluminescence (ECL Western blot Detection Kit; GE Healthcare, Velizy, France). The reactive proteins were detected and analyzed using the ChemiDoc MP System (Bio-Rad, Dusseldorf, Germany).

For analysis and graphical representations (Figure 2, E and G, and Supplemental Table S1), protein bands from immunoblots were quantified using ImageJ software (National Institutes of Health, Bethesda, MD). After subtraction of the background, relative detection levels for modification-specific antibodies were determined by adjusting the values to total tubulin levels (measured with αtot antibody). To determine the status of modifications in the brain (Figure 2G), tissues and HEK293T cells expressing each modified mCherry-α tubulin were coanalyzed (in the same immunoblots; Supplemental Figure S2). This allowed us to determine the sensitivity of each modification-specific antibody in the experiment, which is the ratio of signal with modification-specific antibody to signal αtot obtained with the corresponding modified mCherry-α tubulin. Then signals obtained with tissues extracts were normalized to total α tubulin levels (αtot immunoblot of tissues) and to antibody sensitivity in the experiment. We postulated that the sum of the four analyzed modifications (αTyr, αdeTyr, αΔ2, and αΔ3) represents 100% of α-tubulin in the neonate brain and used bar diagrams to plot results as percentages.

Immunocytochemistry

For immunofluorescence, fibroblasts were fixed at 37°C in 4% paraformaldehyde/4.2% sucrose/PBS, followed by permeabilization in 0.1% Triton X-100/PBS. Neurons were fixed at 37°C in 4% paraformaldehyde, 4% sucrose, 0.25% glutaraldehyde, and 0.1% Triton X-100 and incubated in $NaBH_4$/PBS quenching solution. Cells were then incubated with primary antibodies (Supplemental Table S2), followed by incubation with secondary antibodies conjugated with either cyanine-3 or cyanine-5 fluorophores (1:700–1:1000). Nuclei were stained using Hoescht 33258 (1 μg/ml).

Immunofluorescence analysis

When analyzing immunocytochemistry experiments (Figure 3D), cells were segmented using anti-tyrosinated antibody ($YL_{1/2}$) signal with ImageJ software (Schneider *et al.*, 2012). Cells were classified as GFP positive (mean intensity of 8.8 ± 2.1 and 12.3 ± 2.3, respectively, for CCP1 and CCP5) or GFP negative (mean intensity of 1 ± 0.3). The αΔ3-tubulin content was then expressed as the mean intensity staining for 3EG antibody.

When analyzing neuronal microtubule susceptibility to nocodazole (Figure 6B), the microtubule network was quantified as mean fluorescence intensity measured on lines of 5–15 μm long placed within growth cone of each neuron. In the three conditions (0, 15, and 30 min of nocodazole), 31–60 neurons were analyzed for αTyr and αΔ2 and 49–61 neurons were analyzed for αdeTyr and 3EG. Microtubule fluorescence signal for each variant, *F*(variant), was normalized to αtot signal measured in the same region, *F*(αtot), which is an index of the remaining microtubules), and then was plotted (mean ± SEM) as percentage of the value obtained in the absence of nocodazole.

Immunoprecipitation

Lysates of HEK293T cells were obtained by extraction in 50 mM Tris, pH 8.0, 150 mM NaCl, 1 mM $MgCl_2$, and 20 μg/ml DNase plus protease inhibitors (Complete Mini EDTA-free, Roche Diagnostics, Meylan, France) and 1% NP-40. In the case of neonate brains, soluble proteins were first extracted in the same medium without detergent using a FastPrep apparatus (MP Biomedicals), followed by centrifugation. NP-40 (1%) was added to supernatant containing the brain soluble proteins for immunoprecipitation. Lysates were incubated 2 h at 4°C with either anti–α-tubulin (αtot) or anti–β-tubulin (βtot) antibodies, followed by 1 h of incubation at 4°C with protein G–Sepharose beads (GE Healthcare). Immunoprecipitates were then washed three times with 50 mM Tris, pH 8.0, 150 mM NaCl, and 0.2% NP-40 and directly added to Laemmli solution for analysis. Analyses of the controls (αtot and βtot Western blots) were performed using mouse TrueBlot ULTRA.

Mass spectrometry

Sample preparation. The α- and β-tubulins purified from neonate brain by a cycle of microtubule assembly and disassembly were separated on 10% SDS–PAGE. Protein bands corresponding to β-tubulins were excised and subjected to in-gel proteolytic digestion and proteolytic peptide extraction using the Progest robot (Genomic Solutions, Chemsford, MA). Briefly, bands were extensively washed with acetonitrile and 25 mM NH_4HCO_3 and treated with 10 mM dithiothreitol (30 min at 56°C) and then 55 mM iodoacetamide (30 min at room temperature). Gel slices were then dried and incubated with endoproteinase Asp-N (5 ng/μl; Roche Diagnostics) for 6 h at 37°C. Proteolytic peptides were extracted (using 60% acetonitrile/0.1% formic acid solution, followed by pure acetonitrile), vacuum dried, and resuspended in 5% acetonitrile and 0.1% trifluoroacetic acid before mass spectrometry analysis.

Nano–liquid chromatography/tandem mass spectrometry analysis. Nano–liquid chromatography/tandem mass spectrometry (nanoLC-MS/MS) analyses were performed with the LTQ Orbitrap Velos mass spectrometer (Thermo Scientific) coupled to the EASY nLC II high-performance liquid chromatography system (Proxeon, Thermo Scientific, Waltham, MA). Peptide separation was performed on a reverse-phase C18 column (100-μm inner diameter, 5-μm C18 particles, 15-cm length, NTCC-360/100-5) from Nikkyo Technos (Tokyo, Japan) with a 5–35% solvent B gradient over 40 min. Solvent A was 0.1% formic acid in water, and solvent B was 0.1% formic acid in 100% acetonitrile. NanoLC-MS/MS experiments were conducted in data-dependent acquisition mode. The 20 most intense ions—above an intensity threshold of 2000 counts—were selected for CID fragmentation and analysis in the LTQ. The *m/z* values of the precursor peptide ions were measured with a high resolution of 60,000 in the Orbitrap.

Data analysis. NanoLC-MS/MS data were analyzed in two steps. First, data were processed automatically using the Mascot search engine (version 2.4.1; Matrix Science, London, United Kingdom) in Proteome Discoverer 1.4 against the Swissprot database (release 2014_08), with carbamidomethylation of cysteines as fixed modification and oxidation of methionines and glutamylation of glutamates as variable modifications. Second, a targeted search was conducted against a database composed of all β-tubulin isotypes and all possible C-terminal truncated β-tubulin sequences, with the same modifications as the first search. Peptide and fragment tolerance were respectively set at 10 ppm and 0.6 Da.

ACKNOWLEDGMENTS

We thank Charlotte Corrao and Irene Perez Diez for technical assistance and the zoo technicians for animal care. We are grateful to Jean-Christophe Deloulme for excellent guidance and experimental support on brain dissections and Didier Job for initiation of the project and instructive discussions. We thank Bénédicte Delaval and Anne Fourest-Lieuvin for constructive comments on the manuscript. This work was supported by Association pour la Recherche sur le Cancer Grant SFI20111204053 (M.J.M.) and La Ligue contre le Cancer comité de Savoie (M.J.M.).

REFERENCES

Alexander JE, Hunt DF, Lee MK, Shabanowitz J, Michel H, Berlin SC, MacDonald TL, Sundberg RJ, Rebhun LI, Frankfurter A (1991). Characterization of posttranslational modifications in neuron-specific class III beta-tubulin by mass spectrometry. Proc Natl Acad Sci USA 88, 4685–4689.

Audebert S, Desbruyeres E, Gruszczynski C, Koulakoff A, Gros F, Denoulet P, Edde B (1993). Reversible polyglutamylation of alpha- and beta-tubulin and microtubule dynamics in mouse brain neurons. Mol Biol Cell 4, 615–626.

Baas PW, Ahmad FJ, Pienkowski TP, Brown A, Black MM (1993). Sites of microtubule stabilization for the axon. J Neurosci 13, 2177–2185.

Badin-Larcon AC, Boscheron C, Soleilhac JM, Piel M, Mann C, Denarier E, Fourest-Lieuvin A, Lafanechere L, Bornens M, Job D (2004). Suppression of nuclear oscillations in Saccharomyces cerevisiae expressing Glu tubulin. Proc Natl Acad Sci USA 101, 5577–5582.

Berezniuk I, Lyons PJ, Sironi JJ, Xiao H, Setou M, Angeletti RH, Ikegami K, Fricker LD (2013). Cytosolic carboxypeptidase 5 removes alpha- and gamma-linked glutamates from tubulin. J Biol Chem 288, 30445–30453.

Berezniuk I, Vu HT, Lyons PJ, Sironi JJ, Xiao H, Burd B, Setou M, Angeletti RH, Ikegami K, Fricker LD (2012). Cytosolic carboxypeptidase 1 is involved in processing alpha- and beta-tubulin. J Biol Chem 287, 6503–6517.

Best D, Warr PJ, Gull K (1981). Influence of the composition of commercial sodium dodecyl sulfate preparations on the separation of alpha- and beta-tubulin during polyacrylamide gel electrophoresis. Anal Biochem 114, 281–284.

Bieling P, Kandels-Lewis S, Telley IA, van Dijk J, Janke C, Surrey T (2008). CLIP-170 tracks growing microtubule ends by dynamically recognizing composite EB1/tubulin-binding sites. J Cell Biol 183, 1223–1233.

Brown A, Li Y, Slaughter T, Black MM (1993). Composite microtubules of the axon: quantitative analysis of tyrosinated and acetylated tubulin along individual axonal microtubules. J Cell Sci 104, 339–352.

Cai D, McEwen DP, Martens JR, Meyhofer E, Verhey KJ (2009). Single molecule imaging reveals differences in microtubule track selection between Kinesin motors. PLoS Biol 7, e1000216.

Contin MA, Arce CA (2000). Tubulin carboxypeptidase/microtubules association can be detected in the distal region of neural processes. Neurochem Res 25, 27–36.

Dunn S, Morrison EE, Liverpool TB, Molina-Paris C, Cross RA, Alonso MC, Peckham M (2008). Differential trafficking of Kif5c on tyrosinated and detyrosinated microtubules in live cells. J Cell Sci 121, 1085–1095.

Edde B, Rossier J, Le Caer JP, Desbruyeres E, Gros F, Denoulet P (1990). Posttranslational glutamylation of alpha-tubulin. Science 247, 83–85.

Erck C, Peris L, Andrieux A, Meissirel C, Gruber AD, Vernet M, Schweitzer A, Saoudi Y, Pointu H, Bosc C, *et al.* (2005). A vital role of tubulin-tyrosine-ligase for neuronal organization. Proc Natl Acad Sci USA 102, 7853–7858.

Ersfeld K, Wehland J, Plessmann U, Dodemont H, Gerke V, Weber K (1993). Characterization of the tubulin-tyrosine ligase. J Cell Biol 120, 725–732.

Giraudel A, Lafanechere L, Ronjat M, Wehland J, Garel JR, Wilson L, Job D (1998). Separation of tubulin subunits under nondenaturing conditions. Biochemistry 37, 8724–8734.

Janke C, Bulinski JC (2011). Post-translational regulation of the microtubule cytoskeleton: mechanisms and functions. Nat Rev Mol Cell Biol 12, 773–786.

Janke C, Rogowski K, Wloga D, Regnard C, Kajava AV, Strub JM, Temurak N, van Dijk J, Boucher D, van Dorsselaer A, *et al.* (2005). Tubulin polyglutamylase enzymes are members of the TTL domain protein family. Science 308, 1758–1762.

Kaul N, Soppina V, Verhey KJ (2014). Effects of alpha-tubulin K40 acetylation and detyrosination on kinesin-1 motility in a purified system. Biophys J 106, 2636–2643.

Lacroix B, van Dijk J, Gold ND, Guizetti J, Aldrian-Herrada G, Rogowski K, Gerlich DW, Janke C (2010). Tubulin polyglutamylation stimulates spastin-mediated microtubule severing. J Cell Biol 189, 945–954.

Lafanechere L, Courtay-Cahen C, Kawakami T, Jacrot M, Rudiger M, Wehland J, Job D, Margolis RL (1998). Suppression of tubulin tyrosine ligase during tumor growth. J Cell Sci 111, 171–181.

Lafanechere L, Job D (2000). The third tubulin pool. Neurochem Res 25, 11–18.

Liao G, Gundersen GG (1998). Kinesin is a candidate for cross-bridging microtubules and intermediate filaments. Selective binding of kinesin to detyrosinated tubulin and vimentin. J Biol Chem 273, 9797–9803.

Luduena RF (2013). A hypothesis on the origin and evolution of tubulin. Int Rev Cell Mol Biol 302, 41–185.

Mary J, Redeker V, Le Caer JP, Prome JC, Rossier J (1994). Class I and IVa beta-tubulin isotypes expressed in adult mouse brain are glutamylated. FEBS Lett 353, 89–94.

Miller LM, Menthena A, Chatterjee C, Verdier-Pinard P, Novikoff PM, Horwitz SB, Angeletti RH (2008). Increased levels of a unique post-translationally modified betaIVb-tubulin isotype in liver cancer. Biochemistry 47, 7572–7582.

Moutin MJ, Andrieux A, Janke C (2011). Microtubule polyglutamylation and neurodegeneration [in French]. Med Sci (Paris) 27, 464–467.

Multigner L, Pignot-Paintrand I, Saoudi Y, Job D, Plessmann U, Rudiger M, Weber K (1996). The A and B tubules of the outer doublets of sea urchin sperm axonemes are composed of different tubulin variants. Biochemistry 35, 10862–10871.

Paturle L, Wehland J, Margolis RL, Job D (1989). Complete separation of tyrosinated, detyrosinated, and nontyrosinatable brain tubulin subpopulations using affinity chromatography. Biochemistry 28, 2698–2704.

Paturle-Lafanechere L, Edde B, Denoulet P, Van Dorsselaer A, Mazarguil H, Le Caer JP, Wehland J, Job D (1991). Characterization of a major brain tubulin variant which cannot be tyrosinated. Biochemistry 30, 10523–10528.

Paturle-Lafanechere L, Manier M, Trigault N, Pirollet F, Mazarguil H, Job D (1994). Accumulation of delta 2-tubulin, a major tubulin variant that cannot be tyrosinated, in neuronal tissues and in stable microtubule assemblies. J Cell Sci 107, 1529–1543.

Peris L, Thery M, Faure J, Saoudi Y, Lafanechere L, Chilton JK, Gordon-Weeks P, Galjart N, Bornens M, Wordeman L, *et al.* (2006). Tubulin tyrosination is a major factor affecting the recruitment of CAP-Gly proteins at microtubule plus ends. J Cell Biol 174, 839–849.

Peris L, Wagenbach M, Lafanechere L, Brocard J, Moore AT, Kozielski F, Job D, Wordeman L, Andrieux A (2009). Motor-dependent microtubule disassembly driven by tubulin tyrosination. J Cell Biol 185, 1159–1166.

Redeker V (2010). Mass spectrometry analysis of C-terminal posttranslational modifications of tubulins. Methods Cell Biol 95, 77–103.

Redeker V, Melki R, Prome D, Le Caer JP, Rossier J (1992). Structure of tubulin C-terminal domain obtained by subtilisin treatment. The major alpha and beta tubulin isotypes from pig brain are glutamylated. FEBS Lett 313, 185–192.

Redeker V, Rossier J, Frankfurter A (1998). Posttranslational modifications of the C-terminus of alpha-tubulin in adult rat brain: alpha 4 is glutamylated at two residues. Biochemistry 37, 14838–14844.

Redeker V, Rusconi F, Mary J, Prome D, Rossier J (1996). Structure of the C-terminal tail of alpha-tubulin: increase of heterogeneity from newborn to adult. J Neurochem 67, 2104–2114.

Rogowski K, van Dijk J, Magiera MM, Bosc C, Deloulme JC, Bosson A, Peris L, Gold ND, Lacroix B, Grau MB, *et al.* (2010). A family of protein-deglutamylating enzymes associated with neurodegeneration. Cell 143, 564–578.

Rudiger M, Plessman U, Kloppel KD, Wehland J, Weber K (1992). Class II tubulin, the major brain beta tubulin isotype is polyglutamylated on glutamic acid residue 435. FEBS Lett 308, 101–105.

Rudiger A, Rudiger M, Weber K, Schomburg D (1995). Characterization of post-translational modifications of brain tubulin by matrix-assisted laser desorption/ionization mass spectrometry: direct one-step analysis of a limited subtilisin digest. Anal Biochem 224, 532–537.

Schneider CA, Rasband WS, Eliceiri KW (2012). NIH Image to ImageJ: 25 years of image analysis. Nat Methods 9, 671–675.

Schulze E, Asai DJ, Bulinski JC, Kirschner M (1987). Posttranslational modification and microtubule stability. J Cell Biol 105, 2167–2177.

Sirajuddin M, Rice LM, Vale RD (2014). Regulation of microtubule motors by tubulin isotypes and post-translational modifications. Nat Cell Biol 16, 335–344.
Tort O, Tanco S, Rocha C, Bieche I, Seixas C, Bosc C, Andrieux A, Moutin MJ, Xavier Aviles F, Lorenzo J, Janke C (2014). The cytosolic carboxypeptidases CCP2 and CCP3 catalyze posttranslational removal of acidic amino acids. Mol Biol Cell 25, 3017–3027 .
van Dijk J, Rogowski K, Miro J, Lacroix B, Edde B, Janke C (2007). A targeted multienzyme mechanism for selective microtubule polyglutamylation. Mol Cell 26, 437–448.
Vogel P, Hansen G, Fontenot G, Read R (2010). Tubulin tyrosine ligase-like 1 deficiency results in chronic rhinosinusitis and abnormal development of spermatid flagella in mice. Vet Pathol 47, 703–712.
Webster DR, Gundersen GG, Bulinski JC, Borisy GG (1987). Assembly and turnover of detyrosinated tubulin in vivo. J Cell Biol 105, 265–276.
Wehland J, Weber K (1987). Turnover of the carboxy-terminal tyrosine of alpha-tubulin and means of reaching elevated levels of detyrosination in living cells. J Cell Sci 88, 185–203.
Wehland J, Willingham MC (1983). A rat monoclonal antibody reacting specifically with the tyrosylated form of alpha-tubulin. II. Effects on cell movement, organization of microtubules, and intermediate filaments, and arrangement of Golgi elements. J Cell Biol 97, 1476–1490.
Xiao H, El Bissati K, Verdier-Pinard P, Burd B, Zhang H, Kim K, Fiser A, Angeletti RH, Weiss LM (2010). Post-translational modifications to Toxoplasma gondii alpha- and beta-tubulins include novel C-terminal methylation. J Proteome Res 9, 359–372.